JPRS 78092

18 May 1981

China Report

SCIENCE AND TECHNOLOGY

No. 99

FBIS FOREIGN BROADCAST INFORMATION SERVICE

NOTE

JPRS publications contain information primarily from foreign newspapers, periodicals and books, but also from news agency transmissions and broadcasts. Materials from foreign-language sources are translated; those from English-language sources are transcribed or reprinted, with the original phrasing and other characteristics retained.

Headlines, editorial reports, and material enclosed in brackets [] are supplied by JPRS. Processing indicators such as [Text] or [Excerpt] in the first line of each item, or following the last line of a brief, indicate how the original information was processed. Where no processing indicator is given, the information was summarized or extracted.

Unfamiliar names rendered phonetically or transliterated are enclosed in parentheses. Words or names preceded by a question mark and enclosed in parentheses were not clear in the original but have been supplied as appropriate in context. Other unattributed parenthetical notes within the body of an item originate with the source. Times within items are as given by source.

The contents of this publication in no way represent the policies, views or attitudes of the U.S. Government.

PROCUREMENT OF PUBLICATIONS

JPRS publications may be ordered from the National Technical Information Service, Springfield, Virginia 22161. In ordering, it is recommended that the JPRS number, title, date and author, if applicable, of publication be cited.

Current JPRS publications are announced in Government Reports Announcements issued semi-monthly by the National Technical Information Service, and are listed in the Monthly Catalog of U.S. Government Publications issued by the Superintendent of Documents, U.S. Government Printing Office, Washington, D.C. 20402.

Indexes to this report (by keyword, author, personal names, title and series) are available from Bell & Howell, Old Mansfield Road, Wooster, Ohio 44691.

Correspondence pertaining to matters other than procurement may be addressed to Joint Publications Research Service, 1000 North Glebe Road, Arlington, Virginia 22201.

JPRS 78092

18 May 1981

CHINA REPORT

SCIENCE AND TECHNOLOGY

No. 99

CONTENTS

PEOPLE'S REPUBLIC OF CHINA

PHYSICAL SCIENCES

Large Antenna Structure Homologous Optimization Design
(Wang Shenghong, et al; GUTI LIXUE XUEBAO, No 1, 1981) 1

Observatory Names 11 Minor Planets
(XINHUA, 30 Apr 81) 21

'RENMIN RIBAO' Profiles Nanjing Observatory
(XINHUA, 29 Apr 81) 22

Briefs

Major Solar Flare 23

APPLIED SCIENCES

Photographs of Satellite Tracking Station, New Photoelectron Spectroscope Shown
(KEXUE SHIYAN, No 4, 1981) 24

Crossed Molecular Beam Experimental Facility Completed
(Zou Shuying, Wang Peitang; GUANGMING RIBAO, 7 Jan 81)..... 25

Axial Flow Compressor Test Facility Completed
(GUANGMING RIBAO, 7 Jan 81) 26

Briefs

Standard Time-Measuring Device 27
Shanxi Computer Magnetic Disc 27

PUBLICATIONS

Table of Contents of 'KEXUE HUABAO,' No 2, 1981 28

ABSTRACTS

CONSTRUCTION MACHINERY

GONGCHENG JIXIE [CONSTRUCTION MACHINERY AND EQUIPMENT] No 3, 1981.. 31

MECHANICAL ENGINEERING

JIXIE ZHIZAO [MECHANICAL ENGINEERING] No 2, Feb 81 32

SEISMOLOGY

DIZHEN YANJIU [JOURNAL OF SEISMOLOGICAL RESEARCH] No 4, 1980....... 35

UNDERGROUND ENGINEERING

DIXIA GONGCHENG [UNDERGROUND ENGINEERING] 11 Feb 81 37

PHYSICAL SCIENCES

LARGE ANTENNA STRUCTURE HOMOLOGOUS OPTIMIZATION DESIGN

Hubei GUTI LIXUE XUEBAO [ACTA MECHANICA SOLIDA SINICA] No 1, 1981 pp 12-26

[Article by Wang Shenghong [3769 3932 3163], Li Zhiliang [2621 1807 5328], Wang Qinque [3076 0530 1952], Li Kangyuan [2621 1660 0337], and Chen Zhenhua [7115 2182 5478] of Shanghai Science and Technology University: "A Homologous Optimization Design of Large Antenna Structure"]

[Text] Received 20 November 1979

Abstract

This paper presents an optimization method for the antenna structure design problem in which the target function is the weighted r.m.s. deviation of the deflected surface from the best-fit paraboloid. The complicated target function is partially linearized by using the derivative matrix and reduced to a quadratic convex function. This quadratic convex programming problem is then converted to a linear programming problem with an additional condition which can be solved with a modified simplex method. The optimization parameters include member sections, plate thicknesses, joint coordinates and ratio coefficients between member sections. Several numerical examples show that this approach gives satisfactory results.

Along with the rapid technological development of satellite communication, astronautics, radio astronomy and radar, large precision antenna are used widely. Surface precision is the most important technical factor of large antenna structures. The surface deviation of an antenna refers to the weighted root-mean-square surface deflection from the best-fit paraboloid under the influence of loads (antenna self-weight, wind load, temperature variation load, etc). Therefore the optimum design of an antenna should allow the antenna to change its shape from the original ideal paraboloid to another paraboloid under loads. The design that keeps the paraboloid shape of an antenna is called "homologous" design. This paper gives a homologous optimization design of antenna structure. Since direct computation for a large antenna requires long computer time, a key step of the design is the selection of a rapid optimization method. In this work we use a serial method and approach the best solution asymptotically through the optimization of a series of simplified problems (quadratic convex programming problems).

In solving the antenna deflection due to self-weight, Hoerer[1] first proposed the homologous optimization method. However, the formulas given in Ref (1) are applied only to the hinged rod members and the member sections are not constrained to be positive in the optimization, which can therefore lead to unrealistic "mathematical solutions." In this paper the optimization is generalized to include joint coordinates and ratio coefficients of member sections. This procedure not only improves the optimization results but is also more consistent with the actual engineering structure. The inequality constraint in the optimization guarantees that the solutions obtained are realistic "physical solutions." Moreover, we also give here a comprehensive method for dealing with deflections due to wind load and temperature gradient.

I. Best-Fit Paraboloid

For an ideal paraboloid of focal length f with apex at the origin o of the oxyz coordinate system, it can be described by the following equation

$$x^2 + y^2 = 4fz \tag{1}$$

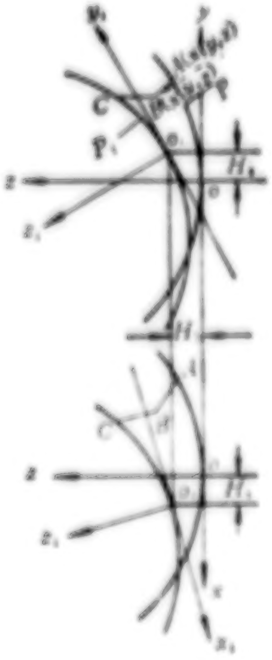

Figure 1

If deflection causes point A on the paraboloid to move to point B through displacement (u,v,w), then the coordinates of point B, $(\bar{x},\bar{y},\bar{z})$, should satisfy the following equation

$$(\bar{x} - u)^2 + (\bar{y} - v)^2 = 4f\,(\bar{z} - w) \tag{2}$$

Consider another paraboloid P_1 with apex o_1 at coordinates (H_1, H_2, H_3). The rotation angle of the axis of P_1, o_1z_1, about the ox-axis is $\theta_x = H_4/2f$ and the rotation angle about oy-axis is $\theta_y = H_5/2f$. Focal length of P_1 is given by $f_1 = f + H_6/2$ and the equation of P_1 in the $o_1x_1y_1z_1$ coordinate system is

$$x_1^2 + y_1^2 = 4(f + \frac{H_6}{2})\, z_1 \tag{3}$$

Since $H_1 \sim H_6$ are small quantities, we can neglect their second order terms. We then have the following coordinate transformation equations

$$\begin{cases} x_1 = x - \dfrac{H_5}{2f} z - H_1 \\ y_1 = y + \dfrac{H_4}{2f} z - H_2 \\ z_1 = z - \dfrac{H_4}{2f} y + \dfrac{H_5}{2f} x - H_3 \end{cases}$$

The equation of P_1 in oxyz can be written as

$$\begin{aligned} x^2 + y^2 = {} & 4fz - 2H_4y + 2H_5x - 4fH_3 + 2H_6z \\ & + \frac{H_5}{f} xz + 2H_1x - \frac{H_4}{f} yz + 2H_2y \end{aligned} \tag{4}$$

From Equations (2) and (4), we obtain the distance $\bar{\delta}$ from point B to surface P_1 along the z direction

$$\bar{\delta} = z - z_1 = \bar{b} - \left(\frac{x}{2f} H_1 + \frac{y}{2f} H_2 - H_3 - (\frac{y}{2f} + \frac{yz}{4f^2}) H_4 + (\frac{x}{2f} + \frac{xz}{4f^2}) H_5 + \frac{z}{2f} H_6\right)$$

where

$$\bar{b} = \frac{x}{2f} u + \frac{y}{2f} v - w \tag{5}$$

Assuming there are n_1 points on the surface, then Equation (5) for these n_1 points can be written in the matrix form

$$\bar{\Delta} = \bar{B} - \bar{V}H \tag{6}$$

where

$$\underset{n_1 \times 1}{\bar{\Delta}} = \left[\bar{\delta}_1,\ \bar{\delta}_2,\ \cdots,\ \bar{\delta}_{n_1}\right]^T$$

$$\underset{n_1 \times 1}{\bar{B}} = \left[\bar{b}_1,\ \bar{b}_2,\ \cdots,\ \bar{b}_{n_1}\right]^T$$

$$\underset{6 \times 1}{H} = [H_1,\ H_2,\ \cdots,\ H_6]^T$$

$$\bar{V} = \begin{pmatrix} \frac{x_1}{2f} & \frac{y_1}{2f} & -1 & -\frac{y_1}{2f}\left(1+\frac{z_1}{2f}\right) & \frac{x_1}{2f}\left(1+\frac{z_1}{2f}\right) & \frac{z_1}{2f} \\ \cdots & \cdots & \cdots & \cdots & \cdots & \cdots \\ \frac{x_i}{2f} & \frac{y_i}{2f} & -1 & -\frac{y_i}{2f}\left(1+\frac{z_i}{2f}\right) & \frac{x_i}{2f}\left(1+\frac{z_i}{2f}\right) & \frac{z_i}{2f} \\ \cdots & \cdots & \cdots & \cdots & \cdots & \cdots \\ \frac{x_{n_1}}{2f} & \frac{y_{n_1}}{2f} & -1 & -\frac{y_{n_1}}{2f}\left(1+\frac{z_{n_1}}{2f}\right) & \frac{x_{n_1}}{2f}\left(1+\frac{z_{n_1}}{2f}\right) & \frac{z_{n_1}}{2f} \end{pmatrix} \tag{7}$$

The square sum of the weighted axial deviation of the n_1 surface points to surface P_1 is

$$D^2 = \sum_{i=1}^{n_1} t_i \bar{\delta}_i^2$$

where $t_i = S_i e_i$ are weighting coefficients, the S_i are area weighting coefficients and the e_i are weighting coefficients for illumination intensity.

Let

$$T = \begin{pmatrix} \sqrt{t_1} & & & \\ & \sqrt{t_2} & \ddots & 0 \\ & 0 & & \sqrt{t_{n_1}} \end{pmatrix}$$

then

$$D^2 = \sum_{i=1}^{n_1} t_i \bar{\delta}_i^2 = (T\bar{\Delta})^T (T\bar{\Delta}) = \Delta^T\Delta = (T\bar{B} - T\bar{V}H)^T (T\bar{B} - T\bar{V}H)$$
$$= B^T B - 2H^T V^T B + H^T V^T V H$$

where

$$\begin{aligned} B &= T\bar{B} \\ V &= T\bar{V} \\ \Delta &= T\bar{\Delta} = B - VH \end{aligned} \tag{8}$$

Let

$$V^T V = Q \tag{9}$$
$$V^T B = P \tag{10}$$

then

$$D^2 = B^T B - 2H^T P + H^T Q H$$

From

$$\frac{\partial D^2}{\partial H_i} = 0 \qquad (i = 1\text{—}6)$$

we obtain the fitting parameter H^* of the best-fit paraboloid

$$\begin{aligned} QH^* &= P \\ H^* &= Q^{-1}P \end{aligned} \tag{11}$$

II. Derivative Matrix M

Assume there are n_2 parameters describing a certain antenna structure, out of which n_3 parameters are to be optimized ($n_3 \leqslant n_2$). Express them as a vector $F = [f_1, f_2, \ldots\ldots, f_{n_3}]^T$. For a given initial structure F_o and degrees of freedom d, the stiffness equation is

$$K_0\delta_0 = P_0 \tag{12}$$

Assume the variation of the parameters is $dF = [df_1, df_2, \ldots\ldots, df_{n_3}]^T$, we then differentiate Equation (12) as follows

$$K_0 d\delta + dK\delta_0 = dP$$

$$\begin{aligned} K_0 d\delta = dP - dK\delta_0 &= \sum_{i=1}^{n_3} \frac{\partial P}{\partial f_i} df_i - \sum_{i=1}^{n_3} \frac{\partial K}{\partial f_i} df_i \delta_0 \\ &= \left[\frac{\partial P}{\partial f_1}, \frac{\partial P}{\partial f_2}, \cdots, \frac{\partial P}{\partial f_{n_3}}\right][df_1, df_2, \cdots, df_{n_3}]^T \\ &\quad - \left[\frac{\partial K}{\partial f_1}\delta_0, \frac{\partial K}{\partial f_2}\delta_0, \cdots, \frac{\partial K}{\partial f_{n_3}}\delta_0\right][df_1, df_2, \cdots, df_{n_3}]^T \end{aligned}$$

Let $$A = \left[\frac{\partial P}{\partial f_1} - \frac{\partial K}{\partial f_1}\delta_0, \frac{\partial P}{\partial f_2} - \frac{\partial K}{\partial f_2}\delta_0, \cdots, \frac{\partial P}{\partial f_{n_3}} - \frac{\partial K}{\partial f_{n_3}}\delta_0\right] \tag{13}$$

then $$d\delta = K_0^{-1} AdF$$

Since we assume that K_0 is the stiffness matrix after the application of boundary conditions, its inverse K_0^{-1} also exists.

Let $$M = K_0^{-1}A \tag{14}$$

we have $$d\delta = MdF \tag{15}$$

Matrix M is known as the "derivative matrix" and it describes the displacement caused by an infinitesimal variation in F. Matrix A is called the "equivalent load derivative matrix" and its ith column is a vector A_i

$$\begin{aligned} A_i = \frac{\partial P}{\partial f_i} - \frac{\partial K}{\partial f_i}\delta_0 &= \frac{\partial}{\partial f_i}\left(\sum_e P_e\right) - \frac{\partial}{\partial f_i}\left(\sum_e K_e\right)\delta_0 \\ &= \sum_e \frac{\partial P_e}{\partial f_i} - \sum_e \frac{\partial K_e}{\partial f_i}\delta_0 \end{aligned} \tag{16}$$

where $\sum_e$ is a sum over all contributing elements. The first term $\frac{\partial P}{\partial f_i}$ represents the load variation caused by changes of parameter f_i; the physical meaning of the second term $\left(-\frac{\partial K}{\partial f_i}\;\partial_0\right)$ is as follows. Changes in parameter

f_i cause changes in the stiffness matrix, so the internal forces will change even if the displacements remain unchanged. The equivalent external load is the resultant of the internal forces on the joint with a negative sign. Once matrix A is formed, we can obtain matrix M by solving Equation (14).

We shall now discuss the equivalent load derivative vector A_i for a few typical cases:

1. Using cross-sectional area of hinged member as optimization parameter

Let the two ends of member e be designated by j and k and assume the member section belongs to the ith optimization parameter f_i. We further assume that external loads consist of self-weight and wind load and the direction of the weight is -y when the antenna is pointed horizontally. Obviously the load contributions of member e are limited to the weight loads at joints j and k:

$$\begin{cases} P_e[3l-2]=0 \\ P_e[3l-1]=-\frac{1}{2}\gamma l_e f_i \\ P_e[3l]=0 \qquad\qquad (l=j,\ k) \end{cases}$$

where γ is the specific gravity, ℓ_e is the length of member e, $P_e[3\ell-2]$ is the contribution at joint ℓ along the x-direction, and so on. Thus,

$$\frac{\partial P_e[3l-1]}{\partial f_i}=-\frac{1}{2}\gamma l_e \qquad\qquad (l=j,\ k) \tag{17}$$

and the remaining terms are zero.

The unit stiffness of the hinged member is

$$[K_e]=\begin{array}{c|cc} & j & k \\ \hline j & C_{jj} & C_{jk} \\ k & C_{kj} & C_{kk} \end{array}$$

where $$C_{jj}=C_{kk}=-C_{jk}=-C_{kj}=\frac{Ef_i}{l_e}\begin{bmatrix} \lambda^2 & \lambda\mu & \lambda\nu \\ \lambda\mu & \mu^2 & \mu\nu \\ \lambda\nu & \mu\nu & \nu^2 \end{bmatrix}$$

and λ, μ, ν are the direction cosines of the member. Hence,

$$\frac{\partial K_e}{\partial f_i}=\begin{bmatrix} C'_{ij} & C'_{jk} \\ C'_{kj} & C'_{kk} \end{bmatrix} \tag{18}$$

where $$C'_{jj}=C'_{kk}=-C'_{jk}=-C'_{kj}=\frac{E}{l_e}\begin{bmatrix} \lambda^2 & \lambda\mu & \lambda\nu \\ \lambda\mu & \mu^2 & \mu\nu \\ \lambda\nu & \mu\nu & \nu^2 \end{bmatrix}$$

Substituting (17) and (18) into (16), we obtain the contribution of member e to the equivalent load derivative vector A_i. When there are more than one member belonging to the ith parameter f_i, their contributions should be added in computing A_i.

2. Using thickness of flat stress plate as optimization parameter

We shall use a rectangular plate to illustrate this case. We designate the corners of the plate element e be h, j, k and m, and assume the plate thickness belongs to the ith optimization parameter f_i. We again assume the external loads being the weight in the -y direction and the wind load. Load contributions of plate e are limited to the weight loads at joints h, j, k and m:

$$\begin{cases} P_e(3l-2) = 0 \\ P_e(3l-1) = -\frac{1}{4}\gamma abf_i \qquad (l = h, j, k, m) \\ P_e(3l) = 0 \end{cases}$$

where a and b are the lengths of the rectangle, as shown in Figure 2.

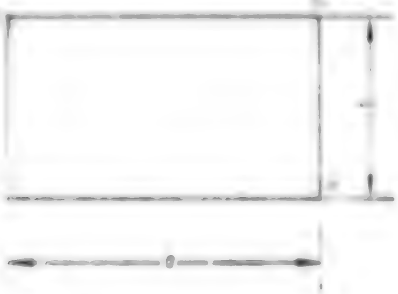

Figure 2

Thus, we have

$$\frac{\partial P_e(3l-1)}{\partial f_i} = -\frac{1}{4}\gamma ab \quad (l = h, j, k, m) \tag{19}$$

and the remaining terms are zero. Also, the unit stiffness of the plate element is

$$[K_e] = [T]^T[\bar{K}_e][T] = \frac{Ef_i}{1-\mu^2}[T]^T[C_e][T]$$

where [T] is the coordinate transformation matrix and $[\bar{K}_e]$ is the unit stiffness of the element in the local coordinate system:

$$[\bar{K}_e] = \frac{Ef_i}{1-\mu^2}[C_e]$$

In the above equation $[C_e]$ is a function of the joint coordinates only. Hence,

$$\frac{\partial K_e}{\partial f_i} = \frac{E}{1-\mu^2}[T]^T[C_e][T] \tag{20}$$

Substituting Equations (19) and (20) into (16), we obtain the contribution of the flat stress plate to the equivalent load derivative vector. If more than one plates belong to the ith parameter f_i, their contributions should be added.

5. Considering temperature difference load in addition to weight and wind

Since the stiffness matrix is independent of temperature, the term $(-\frac{\partial K}{\partial f_i}\delta_1)$ remains unchanged. The effect of the temperature difference $\frac{\partial P}{\partial f_i}$ can be taken into account in the following manner. In the case of a hinged rod let the two ends of the rod member e be designated j and k, and assume the member section is the optimization parameter f_i, then the load contributions of member e due to temperature difference are limited to the joints j and k:

$$\begin{Bmatrix} P_{ej} \\ P_{ek} \end{Bmatrix} = E\alpha T f_i (-\lambda_e \quad -\mu_e \quad -\nu_e \quad \lambda_e \quad \mu_e \quad \nu_e)^T \tag{21}$$

where $T = (T_j + T_k)/2$ is the average temperature, α is the coefficient of expansion. Hence,

$$\begin{Bmatrix} \frac{\partial P_{ej}}{\partial f_i} \\ \frac{\partial P_{ek}}{\partial f_i} \end{Bmatrix} = E\alpha T (-\lambda_e \quad -\mu_e \quad -\nu_e \quad \lambda_e \quad \mu_e \quad \nu_e)^T \tag{22}$$

6. Structures with the requirement that one member section f_A being proportional to another member section f_i.

In this case we have $f_A = f_j f_i$ where the ratio coefficient f_j is also an optimization parameter. In forming Λ_i, one needs to consider the direct contributions from members in f_i as well as those in f_A. If the cross sectional area of member e is in f_A, then

$$\frac{\partial P_e}{\partial f_i} = f_{jA} \frac{\partial P_e}{\partial f_A} \tag{23}$$

$$\frac{\partial K_e}{\partial f_i} = f_{jA} \frac{\partial K_e}{\partial f_A} \tag{24}$$

in which f_{jA} is the ratio coefficient in the previous optimization. Λ_j can be formed according to the following equations

$$\frac{\partial P_e}{\partial f_j} = \frac{\partial P_e}{\partial f_A} \frac{\partial f_A}{\partial f_j} = \frac{\partial P_e}{\partial f_A} f_i \tag{25}$$

$$\frac{\partial K_e}{\partial f_j} = \frac{\partial K_e}{\partial f_A} \frac{\partial f_A}{\partial f_j} = \frac{\partial K_e}{\partial f_A} f_i \tag{26}$$

The optimization of the ratio coefficient f_j has practical significance in antenna structure engineering. For instance, in a spider antenna the members corresponding to the radial girders are generally of equal area. Some radial girders, however, are also supported by secondary surface braces and the forces are more concentrated. It is therefore advisable to enlarge the member section for these girders in designing the antenna.

3. Using joint coordinates as optimization parameters

Consider a hinged member with only weight and wind loads. Let the two ends be i and j and use the z coordinate of joint i as optimization parameter (x and y coordinates can be treated in similar manner).

$$l_e^2 = (x_j - x_i)^2 + (y_j - y_i)^2 + (z_j - z_i)^2$$

$$\frac{\partial l_e}{\partial z_i} = \frac{-(z_j - z_i)}{l_e} = -\nu$$

Load contributions of member e are

$$P_e(3l-2) = 0$$

$$P_e(3l-1) = -\frac{1}{2}\gamma f_e l_e \qquad (l = i, j)$$

$$P_e(3l) = 0$$

hence

$$\frac{\partial P_e(3l-1)}{\partial z_i} = \frac{1}{2}\gamma f_e \nu \tag{27}$$

The unit stiffness of member e is:

$$[K_e] = \begin{bmatrix} C_{ii} & C_{ij} \\ C_{ji} & C_{jj} \end{bmatrix}$$

$$\frac{\partial C_{ii}}{\partial z_i} = \frac{\partial C_{jj}}{\partial z_i} = -\frac{\partial C_{ij}}{\partial z_i} = -\frac{\partial C_{ji}}{\partial z_i} = \frac{\partial}{\partial z_i}\left\{\frac{E f_e}{l_e}\begin{bmatrix} \lambda^2 & \lambda\mu & \lambda\nu \\ \mu\lambda & \mu^2 & \mu\nu \\ \nu\lambda & \nu\mu & \nu^2 \end{bmatrix}\right\}$$

$$= \frac{E f_e}{l_e^2}\begin{bmatrix} 3\lambda^2\nu & 3\lambda\mu\nu & 3\lambda\nu^2 - \lambda \\ 3\lambda\mu\nu & 3\mu^2\nu & 3\mu\nu^2 - \mu \\ 3\lambda\nu^2 - \lambda & 3\mu\nu^2 - \mu & 3\nu^3 - 2\nu \end{bmatrix} \tag{28}$$

Substituting (27) and (28) into (15), we obtain the contribution of member e to the equivalent load derivative vector corresponding to z_i. If the z coordinates of a group of joints are in the same optimization parameter, it is only necessary to add the contributions of all members connected to any joint in that group. The above equations can easily be extended to the cases where changes are in the x and y coordinates.

III. Approximate Expressions of the Target Function

Target function may include the following four situations:

(1) Weighted square sum D_1^2 of self-weight deflection with antenna facing the zenith (Ω = 1 condition);

(2) Weighted square sum D_2^2 of self-weight deflection with antenna pointed horizontally (Ω = 2 condition);

(3) Weighted square sum D_3^2 of self-weight and wind load deflection at elevation angle γ_1 (Ω = 3 condition);

(4) Weighted square sum D_4^2 of self-weight and wind load deflection at elevation angle γ_2 (Ω = 4 condition).

In each of the above cases, preadjustment of self-weight deflection at elevation angle γ_0 should be made. Target function T is given by

$$T = \sum_{i=1}^{4} \eta_i D_i^2 \tag{29}$$

where the weighting coefficients η_i take into account the fact that precision requirements are not exactly the same for the four cases. If their respective r.m.s. accuracy requirements are $[D_i]$, then η_i can be taken as

$$\eta_i = \frac{\sum_{j=1}^{4} [D_j]^2 - [D_i]^2}{3\sum_{j=1}^{4} [D_j]^2}$$

η_i can be chosen more appropriately if we consider the fact that weight effect is always present but effects of wind and temperature are random. When the deformations due to wind and temperature are not included in the target function, then $\eta_3 = \eta_4 = 0$.

1. Ω = 1 and Ω = 2 Condition

(1) Self-weight deflection before parameter variation

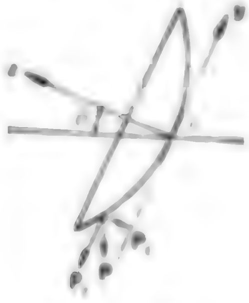

Figure 3

For an arbitrary elevation angle β, the weight of the antenna **P** can be resolved into two components, P_1 parallel to the antenna axis and P_2 in a plane normal to the axis.

$$P = P_1 + P_2$$

For an elevation angle β, we have

$$P_0(\beta) = P_{10} \sin\beta + P_{20} \cos\beta$$

where P_{10} is the self-weight load of the antenna pointed vertically and P_{20} is the self-weight load of the antenna pointed horizontally. The self-weight deflection δ_0 for elevation angle β is

$$\delta_0(\beta) = \delta'_{10} \sin\beta + \delta_{20} \cos\beta$$

in which δ'_{10}, δ_{20} are respectively the vertical and horizontal self-weight deflection. To preadjust for the self-weight deflection at γ_0, the adjustment is

$$\delta_p = \delta'_{10} \sin\gamma_0 + \delta_{20} \cos\gamma_0$$

Hence the actual deflection for arbitrary elevation angle β is

$$\delta_e(\beta) = \delta_0(\beta) - \delta_p = \delta'_{10}(\sin\beta - \sin\gamma_0) + \delta_{20}(\cos\beta - \cos\gamma_0) \tag{30}$$

For the $\Omega = 1$ case, self-weight deflection is

$$\delta_{10} = \xi_1 \delta'_{10} + \xi_2 \delta_{20} \tag{31}$$

in which

$$\xi_1 = 1 - \sin\gamma_0 \qquad \xi_2 = -\cos\gamma_0 \tag{32}$$

For the $\Omega = 2$ case, self-weight deflection is

$$\delta_{20} = \xi_3 \delta'_{10} + \xi_4 \delta_{20} \tag{33}$$

in which

$$\xi_3 = -\sin\gamma_0 \qquad \xi_4 = 1 - \cos\gamma_0 \tag{34}$$

(3) Fitting parameters $H1_\Omega$ ($\Omega = 1$) and $H2_\Omega$ ($\Omega = 2$) before parameter correction

(a) Forming $B1_\Omega$ ($\Omega = 1$) and $B2_\Omega$ ($\Omega = 2$)

From Equation (5), we have

$$B1_0(i) = \frac{x(i)}{2f} u1_0(i) + \frac{y(i)}{2f} v1_0(i) - w1_0(i) \tag{35}$$

$$B2_0(i) = \frac{x(i)}{2f} u2_0(i) + \frac{y(i)}{2f} v2_0(i) - w2_0(i) \tag{36}$$

where $u1'_0(i)$, $u2'_0(i)$, ...are computed from (31) and (33). Combining with (31), (33) and [illegible]

$$\bar{B}1'_0(i) = \frac{u(i)}{2f} u1'_0(i) + \frac{v(i)}{2f} v1'_0(i) - w1'_0(i)$$

$$\bar{B}2'_0(i) = \frac{u(i)}{2f} u2'_0(i) + \frac{v(i)}{2f} v2'_0(i) - w2'_0(i)$$

then

$$\bar{B}1_0 = \xi_1 \bar{B}1'_0 + \xi_2 \bar{B}2'_0$$
$$\bar{B}2_0 = \xi_2 \bar{B}1'_0 + \xi_1 \bar{B}2'_0$$

(b) Forming $\Delta 1_0$, $\Delta 2_0$

Based on Equation (8), let $B1_0 = T\bar{B}1_0$ $\quad B2_0 = T\bar{B}2_0$

then $\Delta 1_0 = B1_0 - VH1_0$ $\quad \Delta 2_0 = B2_0 - VH2_0$

(c) Forming $P1_0$, $P2_0$

Based on Equation (10), let $P1_0 = V^T B1_0$ $\quad P2_0 = V^T B2_0$

(d) Finding fitting parameters $H1_0^*$ and $H2_0^*$

According to Equation (11) $H1_0^* = Q^{-1} P1_0$ $\quad H2_0^* = Q^{-1} P2_0$

(3) Forming derivative matrices M1 and M2

(a) Using Equation (14), form parameter correction matrices M'_1 and M'_2 for the simple self-weight load of a vertical and a horizontal antenna.

(b) After parameter corrections are made, the displacements under self-weight for a vertical and a horizontal antenna are δ'_1 and δ'_2 respectively (without preadjustment). According to (15),

$$\begin{cases} d\delta'_1 = M'_1 dF \\ d\delta'_2 = M'_2 dF \end{cases}$$

$$\begin{cases} \delta'_1 = \delta'_{10} + d\delta'_1 = \delta'_{10} + M'_1 dF & (37) \\ \delta'_2 = \delta'_{20} + d\delta'_2 = \delta'_{20} + M'_2 dF & (38) \end{cases}$$

Here the nonlinear relation between the parameter variation and the displacement variation is linearized by the first order derivatives.

(c) After preadjustment, the displacements under self-weight for vertical and horizontal antenna are δ_1 and δ_2

$$\begin{cases} \delta_1 = \xi_1 \delta'_1 + \xi_2 \delta'_2 \\ \delta_2 = \xi_2 \delta'_1 + \xi_1 \delta'_2 \end{cases}$$

With (37) and (38), we have

$$\begin{cases} \delta_i = \xi_i\Delta_i + \xi_i M_i dF = \xi_i\delta_{i0} + \xi_i M_i dF \\ \delta_j = \xi_j\delta_j + \xi_j M_j dF = \xi_j\delta_{j0} + \xi_j M_j dF \end{cases}$$

Let
$$\begin{cases} M_i = \xi_i M'_i + \xi_i M''_i \\ M_j = \xi_j M'_j + \xi_j M''_j \end{cases} \qquad \begin{matrix}(39)\\(40)\end{matrix}$$

$$\begin{cases} d\delta_i = \delta_i - \delta_{i0} \\ d\delta_j = \delta_j - \delta_{j0} \end{cases}$$

then
$$\begin{cases} d\delta_i = M_i dF \\ d\delta_j = M_j dF \end{cases} \qquad \begin{matrix}(41)\\(42)\end{matrix}$$

Equations (39) and (40) are the derivative matrices under self-weight with preadjustment.

(d) Vectors B_1 and B_2 with parameter correction

From (5) and (41), we have

$$\bar{B}1(i) = \frac{x(i)}{2f}\left(w1_1(i) + \sum_{j=1}^{n_1} M1(3i-2,\ j)dF_j\right)$$

$$+ \frac{y(i)}{2f}\left(w1_2(i) + \sum_{j=1}^{n_1} M1(3i-1,\ j)dF_j\right)$$

$$- \left(w1_3(i) + \sum_{j=1}^{n_1} M1(3i,\ j)dF_j\right)$$

Combining with (35) and (36), we get

$$\bar{B}1(i) = \bar{B}1_0(i) + \sum_{j=1}^{n_1} \bar{C}1(i,j)dF_j$$

where
$$\bar{C}1(i,j) = \frac{x(i)}{2f}M1(3i-2,j) + \frac{y(i)}{2f}M1(3i-1,j) - M1(3i,j)$$

This can be written in matrix form

$$\bar{B}1 = \bar{B}1_0 + \bar{C}1dF \qquad (43)$$

If we let $B1 = T\bar{B}1 \qquad B1_0 = T\bar{B}1_0 \qquad C1 = T\bar{C}1$

then (43) becomes

$$B1 = B1_0 + C1dF \qquad (44)$$

Similarly, for the $\Omega = 2$ case we have

$$B2 = B2_o + C2dF$$

(c) Forming square sums D_1^2 ($\Omega = 1$) and D_2^2 ($\Omega = 2$) after parameter correction

from Equation (8),
$$\begin{cases}\Delta 1 = B1 - VH1 \\ \Delta 2 = B2 - VH2\end{cases}$$
$$D_1^2 = \Delta 1^T \Delta 1 = (B1 - VH1)^T (B1 - VH1)$$
$$= B1^T B1 - 2H1^T V^T B1 + H1^T V^T V H1$$

Substituting (44) into the above expression, we obtain

$$D_1^2 = B1_o^T B1_o + 2B1_o^T C1dF + dF^T C1^T C1dF - 2H1^T V^T B1_o - 2H1^T V^T C1dF + H1^T V^T V H1 \tag{45}$$

Similarly, for the case of $\Omega = 2$, we have

$$D_2^2 = B2_o^T B2_o + 2B2_o^T C2dF + dF^T C2^T C2dF - 2H2^T V^T B2_o - 2H2^T V^T C2dF + H2^T V^T V H2 \tag{46}$$

2. $\Omega = 3$ and $\Omega = 4$ Conditions

For the $\Omega = 3$ case, the counterparts of (31), (39) and (40) are

$$\begin{cases}\delta_{30} = \xi_s \delta'_{1s} + \xi_c \delta'_{2s} + \delta_w \\ M3 = \xi_s M1' + \xi_c M'2 + M3' \\ d\delta_3 = M3dF\end{cases}$$

where $\xi_s = \sin\gamma_1 - \sin\gamma_0$ $\qquad$ $\xi_c = \cos\gamma_1 - \cos\gamma_0$

δ_w is the surface point deflection under wind load only, M3' is the derivative matrix under wind load only and M3 is the derivative matrix under wind and self-weight load.

For $\Omega = 4$, we have

$$\begin{cases}\delta_{40} = \xi_s \delta'_{1s} + \xi_c \delta'_{2s} + \delta_T \\ M4 = \xi_s M'_1 + \xi_c M'_2 + M'_4 \\ d\delta_4 = M4dF\end{cases}$$

where $\xi_s = \sin\gamma_2 - \sin\gamma_0$ $\qquad$ $\xi_c = \cos\gamma_2 - \cos\gamma_0$

δ_T represents the surface point deflection under a temperature difference load only, M'4 is the derivative matrix under a simple temperature load and M4 is the derivative matrix under temperature and weight load. Similarly, the counterparts of (45) and (46) are

$$D_3 = B3_0^T B3_0 + 2B3_0^T C_3 dF + dF^T C_3^T C_3 dF - 2H_3^T V^T B3_0 - 2H_3^T V^T C_3 dF + H_3^T V^T V H_3 \tag{47}$$

$$D_4 = \Delta_4^T \Delta_4 = B4_0^T B4_0 + 2B4_0^T C_4 dF + dF^T C_4^T C_4 dF - 2H_4^T V^T B4_0 - 2H_4^T V^T C_4 dF + H_4^T V^T V H_4 \tag{48}$$

Thus, the approximate expression of the target function after parameter correction is

$$T = \sum_{i=1}^{4} \eta_i D_i = \sum_{i=1}^{4} \eta_i (Bi_0^T Bi_0 + 2Bi_0^T C_i dF + dF^T C_i^T C_i dF - 2H_i^T V^T Bi_0 - 2H_i^T V^T C_i dF + H_i^T V^T V H_i) \tag{49}$$

IV. Recapitulation of the Optimization Problem

The optimization problem requires the target function T given in (49) to approach min! under the condition that the total weight remains constant. The total weight is a function of the optimization parameter:

$$W = W(f_i) \qquad (i = 1 \sim n_1)$$

$$dW = \sum_{i=1}^{n_1} \frac{\partial W}{\partial f_i} df_i$$

Let $\quad a_i = \frac{\partial W}{\partial f_i}$

then the condition of a constant total weight becomes $\quad \sum_{i=1}^{n_1} a_i df_i = 0$

or, in matrix form $\quad AdF = 0$ (50)

where $\quad A = [a_1, a_2, \cdots, a_{n_1}]$ (51)

Considering the engineering aspect of the antenna structure, we further impose the following two conditions:

(1) An inequality constraint is imposed on the optimization parameters. Without losing generality, it can be written as

$$f_i \geqslant g_i \qquad (i = 1 - n_3)$$

or, in vector form $\quad F \geqslant G_2$

Let $dF = F - F_0$, $G = G_A - F_0$, then,

$$dF \geqslant G \tag{52}$$

(2) The fitting parameters H_i $(i = 1 \sim 6)$ are required to be constants. Here one of the following cases can be chosen:

(a) Fitting parameters remain constant throughout the optimization process and their values are taken to be those of the initial structure. In this case an optimization solution closest to the initial structure is approached.

(b) Fitting parameters can change in the optimization process but $(H_i)^{k+1}$ is kept constant in the k+1st iteration of the optimization--its value is taken to be equal to the best-fit parameter $(H_i^*)^k$ in the previous (k th) iteration.

(c) Fitting parameters are zero throughout the optimization process, that is, let the square sum of the absolute deflection be the target function. This is the special case of rigid design.

In all three cases described above H_i is a constant. Dropping the constant term in (49), we have

$$T = \sum_{i=1}^{l} \eta_i (2B_{0i}^T C_i dF - 2H^i V^T C_i dF + dF^T C_i^T C_i dF) \tag{53}$$

and the problem becomes

$$\left.\begin{array}{l} T dF \rightarrow \min! \\ \text{and satisfy} \begin{cases} A dF = 0 \\ dF \geqslant G \end{cases} \end{array}\right\} \tag{54}$$

Let $X = dF - G$, then the problem becomes

$$\left.\begin{array}{l} T = P^T X + X^T C X \rightarrow \min! \\ \text{while satisfying} \begin{cases} AX = B \\ X \geqslant 0 \end{cases} \end{array}\right\} \tag{55}$$

Quantity P^T and matrices C and B are as follows:

$$P^T = \sum_{i=1}^{l} 2\eta_i (B_{0i}^T C_i - H^i V^T C_i + G^T C_i^T C_i)$$

$$C = \sum_{i=1}^{l} \eta_i C_i^T C_i$$

$$B = -AG$$

The $n_f \times n_f$ matrix C is obviously symmetric and positive definite. The problem described by (55) is therefore a programming problem for a quadratic convex function with a linear constraint and a non-negative parameter.

V. Quadratic Convex Programming

In the following quadratic convex programming problem

1)
$$\begin{cases} T = P^TX + X^TCX = \min! \\ AX = B \\ X \geq 0 \end{cases}$$

the necessary and sufficient conditions that vector $X^0 \in R^{n_1} (X^0 \geq 0)$ is the minimum solution of problem (1), according to Kuhn-Tucker condition,[2] are

(a) $AX^0 = B$

(b) there exist vectors $U^0 \in R^{m_1}$ and $V \in R^{n_1}$ satisfying

$$\begin{cases} V^0 - 2CX^0 - A^TU^0 = P \\ V^0 \geq 0 \\ X^{0T}V^0 = 0 \end{cases}$$

Problem (1) can be solved[3] by transforming into the following equivalent problem (2)

2)
$$\begin{cases} AX = B \\ -2CX + V - A^TU + h\xi = P \\ X \geq 0 \qquad V \geq 0 \qquad \xi \geq 0 \\ X^TV = 0 \\ \xi = \min! \end{cases}$$

where $h = P + 2CX_0$, X_0 is the initial solution satisfying $AX = B$ and $X \geq 0$. Here A is real $m_1 \times n_1$ matrix, C is a $n_1 \times n_1$ symmetric and positive-definite matrix and $X, P, V \in R^{n_1}$, $B \in R^{m_1}$.

Problem (2) is a linear programming problem with an additional condition $X^TV = 0$ and can be solved with a "modified simplex method." Since there is no $U \geq 0$ constraint in problem (2), we let

$$U = U_1 - U_2,\ U_1 \geq 0,\ U_2 \geq 0,$$

and (2) is reduced to an ordinary linear programming problem associated with the following matrix

$$\bar{A} = \begin{bmatrix} A & 0 & 0 & 0 & 0 & B \\ -2C & E & -A^T & A^T & h & P \\ 0 & 0 & 0 & 0 & 1 & 0 \\ 0 & 0 & 0 & 0 & 0 & 0 \end{bmatrix}$$

In the above matrix, if B and P have negative components, the entire roll they are in changes sign. Since $m_1 = 1$ in our problem, we can choose the initial solution as

$$X_i = \dot{0} \qquad (i = 1 - n_0 - 1)$$

$$X_{n_0} = \frac{b}{a_{n_0}}$$

We also introduce a signal working element BB[1:N] (with $N = 2(n_0 + m_0 + 1) - 1$) in our computation so that the additional condition $X^TV = 0$ can be realized. For variable x_i (or v_i) and its corresponding v_i (or x_i) in the basis, we choose BB[i] = 0 and BB[i + n_0] = 0 (or, BB[i - n_0] = 0 for i > n_0). We further make the restriction that δ_k can only be found in $\delta_j < 0 \wedge BB[j] \neq 0$ then X^TV is satisfied.

VI. Application Examples

Using the method described here we wrote two computer programs for model TQ-6 and model 719 computers respectively. The target function includes weight deflection preadjusted at 0° and 90° angles of elevation. Although the wind and temperature deflections are not included in the target function in this program, they are computed simultaneously to see if the structure optimized for weight is also satisfactory under wind and temperature loads. The programs are applicable to hinged members and two-dimensional combination plates. Optimization parameter of the program can be member sections, joint coordinates or ratio coefficients. We applied the program to three antenna and obtained satisfactory results.

1. 20-meter antenna

Figure 4 shows the calculation for one-fourth of the 20m antenna structure. The ¼ structure has 58 joints, 180 members (divided into 25 kinds, see Figure 4), 8 triangles and 4 rectangles. The program has 27 optimization parameters including 23 member sections (labelled 1~23 in Figure 4) and 4 joint coordinates (z coordinates of joints A,B,C, and D). After 28 iterations the average value of the weighted r.m.s. deviation for 0° and 90° elevation angles is reduced from 0.1151mm to 0.0167mm. For 0° angle the r.m.s. deviation is reduced from 0.1132mm to 0.0137mm, and for 90° angle the r.m.s. deviation is reduced from 0.1168mm to 0.0204mm. The antenna has high accuracy after optimization. On the 719 computer the total iteration time is 5 hours.

2. Communication satellite ground station antenna

Figure 6 shows the computation for one-fourth of a large antenna. The antenna has a shear-resistant belly-plate center structure and a backstay with spider and ring beams. One-fourth of the antenna has 162 joints, 459 rod members (27 different kinds), 37 triangles and 23 rectangles. For structural and technical reasons there are only 17 optimization parameters, they are all member sections. Technical standard of the antenna requires that at 0° and 90° the r.m.s. weight deflection from the best-fit paraboloid should be less than 0.15mm. Owing to a good initial design the r.m.s. deflections at 0° and 90° are respectively 0.072mm and 0.073mm in the beginning. However, they are reduced further after 23 iterations; the optimized values are 0.057mm and 0.056mm respectively. They are far better than design requirements. On the QT-6 computer,

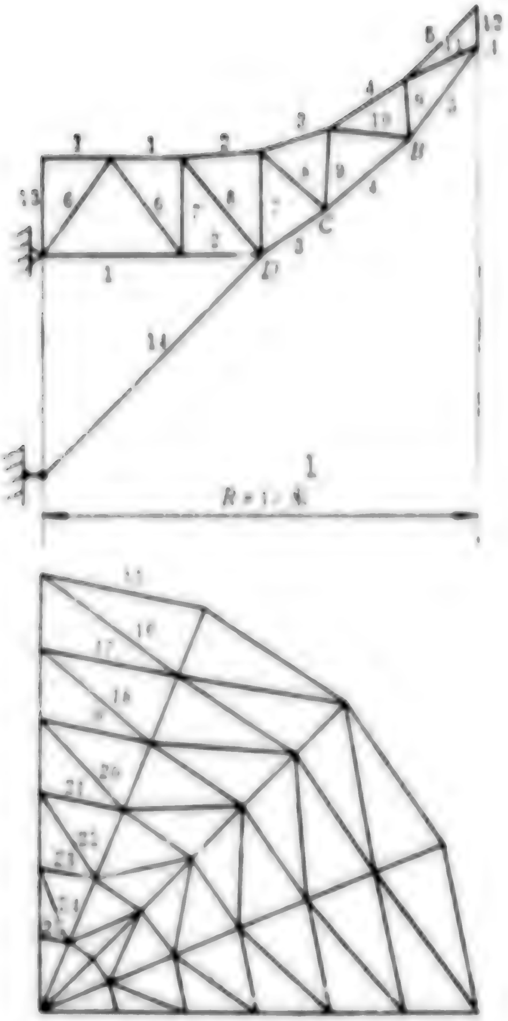

Figure 4

Key: 1. meter

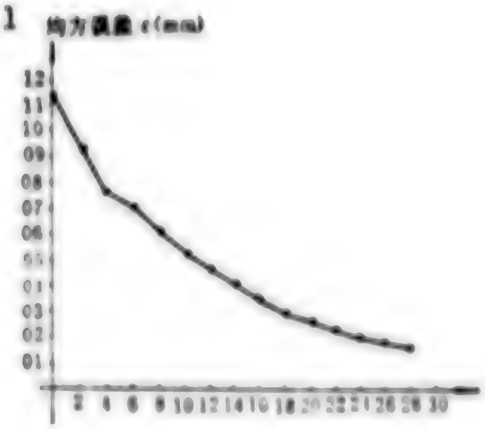

Figure 5

Key: 1. r.m.s. error

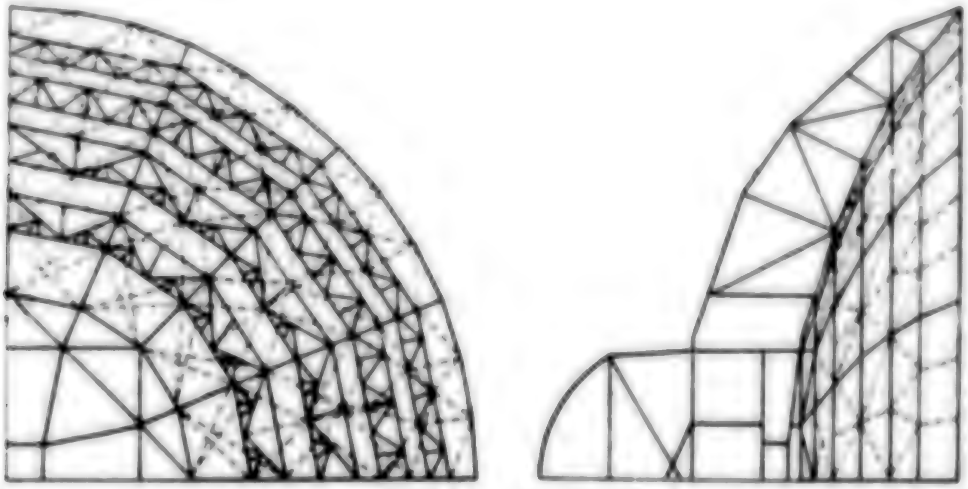

Figure 6

the total optimization time is 4 hours. With finer division of rod members and with more optimization parameter one can expect to gain even higher accuracy, but a sensible choice of the optimized structure should be made with both accuracy and building technique taken into account.

3. 10m antenna

Since this antenna has relatively small diameter, the target function is taken to be the r.m.s. absolute deflection under self-weight from 0° to 90°, that is, a rigid design. One-fourth of the structure has 48 joints, 148 members, 8 triangles and 3 rectangles. There are 24 different kinds of rod members and the sections of 23 of them are used as optimization parameters. After 18 iterations, the r.m.s. absolute deflection under weight at 0° and 90° are reduced respectively from 0.18mm and 0.14mm to 0.12mm and 0.09mm. Three hours of computing time are used on the 719 computer. In the meantime the r.m.s. deviations from the best-fit paraboloid are reduced from 0.031mm and 0.018mm to 0.020mm and 0.012mm for 0° and 90° elevation angles respectively.

REFERENCES

1. V. Hoerer, J. of Structural Division, ASCE, 93, 461-486 (1967).

2. L. Collatz and W. Wetterling, OPTIMIZATION PROBLEMS, pp 235-240, Springer-Verlag, New York, 1975.

9698
CSO: 4008/279

PHYSICAL SCIENCES

OBSERVATORY NAMES 11 MINOR PLANETS

OW301216 Beijing XINHUA in English 1207 GMT 30 Apr 81

[Text] Nanjing, 30 Apr (XINHUA)--The Purple Mountain Observatory in Nanjing has announced the naming of 11 new minor planets it has discovered over the last 17 years, according to a spokesman for the observatory today.

The observatory has been informed by the International Astronomical Union (IAU) that these minor planets have been identified and numbered. The IAU, to verify a discovery, requires three observations by its own scientists.

The prerogative to choose the name of a new minor planet has been traditionally assigned to the discoverer. Consecutive numbers are assigned to the planets whose orbits are accurately known.

The new minor planets are named as follows:

minor planet (2197) discovered on 30 December 1965, 'Shanghai';
minor planet (2209) discovered on 28 October 1978, 'Tianjin';
minor planet (2215) discovered on 12 November 1964, 'Sichuan';
minor planet (2223) discovered on 4 October 1977, 'Himalayas';
minor planet (2230) discovered on 29 October 1978, 'Yunnan';
minor planet (2255) discovered on 3 November 1977, 'Qinghai';
minor planet (2260) discovered on 26 November 1975, 'Kunlun';
minor planet (2263) discovered on 30 October 1978, 'Shaanxi';
minor planet (2336) discovered on 26 November 1975, 'Xinjiang';
minor planet (2344) discovered on 27 September 1979, 'Tibet';
minor planet (2355) discovered on 30 October 1978, 'Inner Mongolia'.

So far the observatory has named 24 minor planets. Five of the previously named 13 minor planets were named after China's ancient astronomers: Zhang Heng, Zu Chongzhi, Yi Xing, Guo Shoujing and Shen Kuo. The rest were named after Chinese places: Beijing, Jiangsu, Nanjing, Henan, Anhui, Taiwan, Fujian and Guangdong.

CSO: 4020/182

'RENMIN RIBAO' PROFILES NANJING OBSERVATORY

OW291310 Beijing XINHUA in English 1259 GMT 29 Apr 81

[Text] Beijing, 29 Apr (XINHUA)--A group of 10 minor planets discovered by the Purple Mountain Observatory in Nanjing have recently been identified by the International Astronomical Union (IAU) and will be named by the observatory, the "PEOPLE'S DAILY" reported today.

Accompanied by nearly half a page of photographs showing the work and achievements of the observatory, the report said the observatory has discovered 13 minor planets since 1949, which have been named after Chinese places and ancient astronomers, and three comets, "Purple Mountain" No 1, 2, and 3.

The first Chinese astronomer to discover a minor planet is 79-year-old Professor Zhang Yuzhe, director of the observatory. The planet he discovered in 1928 is named "Zhonghua (China)."

The observatory, built in 1934 on the picturesque Purple Mountain in Nanjing, was small at its initial stage. It was devastated during the war of resistance against Japan (1937-1945) and its work was at a standstill in 1949.

Now with its solar physics, stellar physics, radio astronomy, space astronomy, artificial satellite, astronomical calculation and other laboratories, the observatory has become one of the most comprehensive and well equipped research institutes in China. Two hundred and fifty astronomers, as opposed to 10 at the time of liberation, now work there.

The astronomers from Purple Mountain, collaborating with their colleagues at the Beijing Observatory, observed on 11 March 1977 the ring of Uranus, a major discovery in astronomical research.

In March 1979 they took an astrophotograph of a ring-shaped solar flare prominence and in September 1980 they photographed a rare H-alpha flare spectrum.

In 1969 the observatory began compiling and publishing China's astronomical calendar and ended reliance on foreign compilation.

CSO: 4020/182

BRIEFS

MAJOR SOLAR FLARE--Nanjing, 29 Apr (XINHUA)--The Zijinshan (Purple Mountain) Observatory in Nanjing, capital of Jiangsu Province, reported sighting a 2-hour major solar explosion on 27 April. The explosion commenced at 3:18 pm (Beijing time), and lasted until 5:24 pm. The explosion's 3.2-centimeter radio radiation flux release was 45 times as great as the normal, while the 10-centimeter radio radiation flux was 22 times as great. The flare is the biggest of its kind sighted by Chinese observatories since the peak year of solar activity which began in September 1979. The Zijinshan Observatory saw the flarelike eruption of solar prominence as soon as the explosion's corresponding sunspot activity area rotated from the sun's western edge. Astronomers at the observatory sighted a third degree solar flare beginning at 7:50 am (Beijing time) on 23 April and a second degree flare beginning at 9:50 am on 24 April. The two big solar flares interrupted short-wave communications. [Text] [OW300149 Beijing XINHUA in English 1229 GMT 29 Apr 81]

CSO: 4020/182

APPLIED SCIENCES

PHOTOGRAPHS OF SATELLITE TRACKING STATION, NEW PHOTOELECTRON SPECTROSCOPE SHOWN

Beijing KEXUE SHIYAN [SCIENTIFIC EXPERIMENT] in Chinese No 4, 1981, inside front cover

[Photo captions]

Shown is the exterior view of the Chinese Academy of Sciences' Guangzhou satellite observation station. Four sets of heavy precision equipment, all designed and built in China, are installed therein.

The first Chinese photoelectron spectroscope has been successfully developed by the Shenyang Scientific Instruments Plant. It can be used for the analysis of the solid, liquid and gaseous states of organic or inorganic substances or powdered samples to provide useful information of the chemical environment on the molecular and atomic energy levels.

CSO: 4008/318

CROSSED MOLECULAR BEAM EXPERIMENTAL FACILITY COMPLETED

Beijing GUANGMING RIBAO in Chinese 7 Jan 81 p 2

[Article by Zou Shuying [6760 3219 5391] and Wang Peitang [3769 1014 2768]: "First Crossed Molecular Beam Experimental Facility Completed in Dalian"]

[Text] China's first general and powerful large-scale crossed molecular beam experimental facility has been completed by the Dalian Chemical Physics Institute, Chinese Academy of Sciences. This facility gives China a powerful research tool for the study of microscopic reaction dynamics.

This experimental facility is a general, multidiscipline instrument equipped with ultrahigh vacuum, supersonic injection, and laser, and is capable of detecting and measuring the spectra, mass spectra, and very weak signals. It can be used to measure the state distribution of various chemical reaction products under single collision conditions, and the angular distribution of luminous chemical reaction products. It can be used to study the effects of the initial energy states of reactants on the reaction process and the phenomenon of photodissociation due to laser. It is further equipped to make measurements of the mass spectra, spectra, laser-induced fluorescence, and chemical imagery.

The technical personnel and workers of the Dalian Chemical Physics Institute began the design and construction of this experimental facility in 1979, and within a period of only 2 years they have completed their task. Using this experimental facility, they have already successfully obtained very good results from an experimental study of microscopic reaction dynamics.

Those who participated in the construction of this experimental facility were all young Chinese scientists.

9113
CSO: 4008/238

APPLIED SCIENCES

AXIAL FLOW COMPRESSOR TEST FACILITY COMPLETED

Beijing GUANGMING RIBAO in Chinese 7 Jan 81 p 2

[Article: "An Axial Flow Compressor Test Facility for Thermophysics Research on Aviation Engines Completed"]

[Text] The Engineering Thermophysics Institute of the Chinese Academy of Sciences has recently completed construction of a modern, transonic, single- and two-stage, axial flow compressor testing facility, and has successfully completed a preliminary test run. The test facility operated normally, and all the design performance indexes have been verified. This test facility is an important piece of equipment for thermophysics research on aviation engines.

The success or failure of an aviation engine hinges to a large extent on the design of its compressor. The gas-thermodynamic design of the transonic compressor is one of the key links of modern aviation engine design. The famous Chinese aerodynamicist and president of the Engineering Thermophysics Institute of the Chinese Academy of Science, Prof Wu Zhonghua [0702 0112 5478], has developed a three-dimensional flow theory around the blades and rotary machinery. His theory has received international recognition and is employed widely in the design of power machinery, including aviation engines, gas turbines, and steam turbines. Wu Zhonghua's three-dimensional flow theory has been further developed theoretically in recent years, but experimental verificiation of the theory could not be carried out in a timely manner due to the lack of an appropriate testing facility. This transonic, single- and two-stage, axial flow compressor experimental facility of the Engineering Thermophysics Institute is expected to provide the necessary conditions for us to understand the complex three-dimensional flow process inside the transonic compressor, and the necessary fundamental design data for the development of newer and more advanced transonic aviation compressors.

All equipment used in the construction of this experimental facility was designed and manufactured in China. This was a result of cooperation among the various units concerned, including the First and the Third Ministry of Machine Building and the Chinese Academy of Sciences.

9113
CSO: 4008/238

BRIEFS

STANDARD TIME-MEASURING DEVICE--Beijing, 23 Apr (XINHUA)--China has successfully made a cesium-beam time-measuring device, filling a gap in its metrological science. This device, based on the frequency of a beam of cesium atoms, has a precision of 8 ten-trillionths of a second; in other words, there would not be a 1-second error for 40,000 years. The achievement is credited to the Chinese Metrological Research institute, which started the project of making such a device in 1969 and succeeded in 1980. [Beijing Xinhua Domestic Service in Chinese 0240 GMT 23 Apr 81]

SHANXI COMPUTER MAGNETIC DISC--Taiyuan, 14 Apr (XINHUA)--The Taiyuan Magnetic Recording Technology Research Institute in Shanxi has successfully developed an RF-1 type 8-inch soft magnetic disc for computers. Among its advantages are its large storage capacity, speediness in storing and retrieving data, handiness, good interchangeability and low price. Recent test by the Fourth Ministry of Machine-Building showed that the disc reached the level of similar products abroad in terms of storage capacity, recording density [ji lu mi du 6068 6922 1378 1653] and error rate. [OW201004 Beijing Xinhua Domestic Service in Chinese 0014 GMT 14 Apr 81]

CSO: 4008/316

TABLE OF CONTENTS OF 'KEXUE HUABAO,' NO 2, 1981

Shanghai KEXUE HUABAO [SCIENCE PICTORIAL] in Chinese No 2, Feb 81 p 48

[Text] Predictions and Prospects

What Do the Scientists Have in Mind?
Zhu Zhangchao [2612 7022 6289] (1)
Mammoth of 40,000 Years Came Back to Life
The Mechanism That Controls Life
All Those Superweapons
Cross Breeding Between Animals and Plants
Grand Plan To Exploit the Moon

Modernization

Breakthrough
Compiled and Translated by Zhang Xinduo [1728 9444 6995] (10)
The Eighth Wonder of the World
Deng Ziyi [6772 1311 1355] (24)
Unveiling the Mystery of Biorhythm--the Up and Down Regularity in Stamina, Emotion and Intelligence
Chen Kang [7115 1660] (6)
How To Measure Your Own Biorhythm
Chen Kang [7115 1660] (7)
New Residents of the Feeding Lot
Lin Zitong [2651 1311 6639] (8)

Outpatient Doctor

Eating Meat Is No Taboo
The Optimum Time for Infants To Have Surgery (14)
"Double Eyelid" and Heredity
Precaution in Treating Ascaris (15)
How To Use Eyedrops Properly
Birth Control Methods for Newlyweds (16)

Nature and Society

Whole Life Talent Design: From Birth to Eighty, Part II
Xu Liyen [6079 4539 6056], Ma Xiaoqing [7456 1420 7230 and
Wang Dunqi [3769 2415 38[illegible]] (3)

"Urban Hazards" and Society Engineering
Xu Liyen [6079 4539 6056] (12)
Twins and Spiritual Connection
Compiled and Translated by Chen Ketong [7115 0344 2768] (22)
Animals With Skill and Animals With Intelligence
Yao Dajun [1202 1129 0971] (28)
The Incident of the Missing Hydrogen Bomb at Pa-lo-mai-li
Lu Xueshi [0712 1331 6108] (42)
Which Memorization Technique Suits You the Best?--First Impression Technique, Adult Memorization Method, Alternating Memorization Technique, and Characteristics Memorization Method
Lei Zhenxiao [7191 4394 1321] and Cao Liang [2580 0081] (26)

Traveling Around the World

Paradise in the East--Korea's Sorak San
Varanasi--the Hindu Holy City (30)
A River That Flows to the Sky
Munich--the Holy Land of Beer (31)

Tidbits in Science

Inspiration of Mrs Potter's Forms
Four Year Old College Student (32)
Library in a Spoon
"Vampire" Bacteria (33)
Camel's Blood Plasma
Precise Memory and Vague Memory (34)

Brain Exercises

Fur Merchant's Clever Sales Pitch
Handshakes at a Party
Altair Meets Vega (36)
Big Gray Wolf Catches a Rabbit
Recognizing the "Hero" (37)

Little Experiments (38)
Saliva That Changes Color
1 + 1 # 2
Star Lights in a Test Tube
Graduated Cylinder That Enhances Sound
New Technique for Taking Pulses
Cellophane Tape That Changes Color
The Vanishing Light Beam
Simple Pendulum Draws Geometric Patterns

The Whys (40)
Why Does Some Gasoline Have Yellow or Red Color?
Why Are Alkaline Soaps Not Suitable for Washing Fabrics Containing Gold and Silver Threads?
Why Can a Blindfolded Owl Still Catch a Mouse?

Why Is It Not Good to Store Cooking Oil in Plastic Containers Over an Extended Period of Time?
Why Is the Blood Blue in the Vein?
Why Is the Number of Jewels in a Watch Always Odd and Never Even?
Why Does Gastric Ulcer Pain Often Occur After a Meal Whereas Duodenal Ulcer Pain Occurs Before a Meal?
Why Are Long Telephone Conversations Hard to Hear?
Why Is It Not Necessary To Check Blood Type Before Transfusion in Livestock?
Why Is Mimosa Not Shy Before It Rains?

Science Fiction (45)
Who Is Running the Election Campaign?
Stephen Robinett (of U.S.A.)

Brief News in Science and Technology
Ultraminiature Electromagnetic Valve
Color Television Live Broadcasting Mobile Unit
Cutting Concrete With Flame
Integrated Infrared Heating Element
Novel Rust Proof for Metallic Surface
Grape Pollen Planting Success
World's Largest Solar Power Station
Fountain Type Negative Ion Generator
Portable Small Boat
Fire Fighting and Rescue Mask
Colored Light and Egg-Laying Hen
Electric Periodic Linear-Travel Motion Mechanism
Multi-Colored Light Emitting Diode
Electricity Consumption Monitor
Aromatic Metals
Another Solar-Powered Aircraft Tested
New Protective Bandage

Front Cover: Huajing Brand Semiconductor Components

Inside Front Cover: What Do the Scientists Have in Mind?

Inside Back Cover: Products of Shanghai Compressor Plant

Back Cover: New Coloring Agent for Polyenic Hydrocarbons

END
CSO: 4008/286

AUTHOR: None

ORG: Zhuzhou Mining Machinery Parts General Plant; Tianshui Research Institute of Pneumatic Tools

TITLE: "YYG-80 Hydraulic Rock Drilling Machine"

SOURCE: Tianjin GONGCHENG JIXIE [CONSTRUCTION MACHINERY AND EQUIPMENT] in Chinese No 3, 81 pp 1-3

ABSTRACT: Hydraulic rock drilling machines are a new type of rock drilling equipment created in the early 70's. Now all countries in the world are competing in their development. Research on their manufacture began in China in 1973 by a joint research group organized by the Zhuzhou Mining Machinery Parts General Plant of the First Ministry of Machines, the Tianshui Research Institute of Pneumatic Tools, the Changsha Research Institute of Mining and Metallurgy of the Ministry of Metallurgy, and East Hunan Tungsten Mine. From Aug 73 to Aug 80, the product, the YYG-80 guide type hydraulic rock drilling machine went through laboratory and industrial tests as well as repeated improvements. A conference held on 23-26 Sep 80 certified it to be preliminarily complete. It will soon be manufactured in batches to be extended in the mining industry. The work theory, the structural characteristics, and the repair and maintenance procedure are discussed. The work process and the structure are illustrated with drawings.

AUTHOR: ZENG Zhaoyou [2582 2507 2589]

ORG: Fushun Excavating Machinery Plant

TITLE: "Brief Introduction of the Improved Design of the W1001 Excavator"

SOURCE: Tianjin GONGCHENG JIXIE [CONSTRUCTION MACHINERY AND EQUIPMENT] in Chinese No 3, 81 pp 3-6

ABSTRACT: The Fushun Excavating Machinery Plant has been producing the W1001 excavators in large quantities for many years. Many customers are familiar with this line of products. Most recently, based upon opinions of the users and merits of similar products made in foreign countries, the author and colleagues proceeded with serious analysis of the original design and made improvements to the chassis, the operating system, and the work performing portion. The various improvements are explained separately and illustrated with drawings.

6248
CSO: 4009/226

AUTHOR: HUANG Mingliang [7806 7686 0081]

ORG: Research Institute of Grinding Machines, Shanghai Machine Tool Plant

TITLE: "Mirror Surface Turning Equipment and Work Process--ST186 High Precision Magnetic Disk Lathe and Diamond Tooling Blade"

SOURCE: Shanghai JIXIE ZHIZAO [MECHANICAL ENGINEERING] in Chinese No 2, Feb 81 pp 3-7

ABSTRACT: Following the rapid development of electronic computer industry, the Research Institute of Grinding Machines proceeded with studying the process of finishing the mirror surface of the magnetic disk--a major component of the external storage unit of computers. The magnetic disk is made of rolled 188 aluminum magnesium titanium beryllium alloy. Originally, the disk had to be turned, ground, polished, etc. requiring 6 hours for each disk. A new process has now been devised to use monocrystalline natural diamond as the cutting tool to finish each disk in 30 minutes to achieve a smoothness of △13c and a 2-surface dissimilarity less than 2 μm. The structural characteristics of the tooling machine and the work requirements are discussed.

AUTHOR: HUANG Hao [7806 3185]

ORG: Baoji Machine Tool Repair Plant

TITLE: "Introducing Intermittent Broaching and Tapping of T40 x 12 Internal Screw Thread"

SOURCE: Shanghai JIXIE ZHIZAO [MECHANICAL ENGINEERING] in Chinese No 2, Feb 81 pp 15-17

ABSTRACT: For the purpose of resolving the problem of finishing the C620-1B lathe opening and closing nut, with T40 x 12 thread and 120mm finishing length, the author and colleagues designed an intermittent broaching and tapping tool. It has been in use since 1974 and proved to be a reasonable, highly efficient, and high quality cutting tool. It is an ideal tool for cutting internal thread of relatively large thread pitch, relatively large diameter, and relatively high precision requirements. The structure of the tool, the function of the various components, and the design parameters are explained.

AUTHOR: None

ORG: Shanghai Colloid Chemical Plant

TITLE: "A New Lubricant--Forging Press Graphite Oil Supplied by Shanghai Colloid Chemical Plant"

SOURCE: Shanghai JIXIE ZHIZAO [MECHANICAL ENGINEERING] in Chinese No 2, Feb 81 pp 34-35

ABSTRACT: At present, many synthetic lubricants for hot press forging are available in foreign countries. They have good lubricating property under high temperature and are good for discharging products, cooling, and heat insulation as well. They include the Delta-144 of Acheson Company of W. Germany, the Dag-31 of the USA, etc. and all are forms of graphite oil. In China, a mixture of graphite powder, machine oil, cylinder oil, saline solution, and soap solution, based upon an oil formula of the USSR, had always been used. For forging press, this lubricant is useable but it creates a great deal of smoke and flame, which are injurious to the workers and often causes large pieces of forged products to be difficult to separate from the mold. It was not until 1977 when Shanghai Colloid Chemical Plant finally succeeded in making the graphite oil lubricant. This paper compares its properties with those of the aforementioned foreign products and explains the composition of this type of lubricants.

AUTHOR: HUANG Yue [7806 1971]

ORG: China Phonographic Record Company

TITLE: "Comprehensive Utilization of Electrolysis Sludge"

SOURCE: Shanghai JIXIE ZHIZAO [MECHANICAL ENGINEERING] in Chinese No 2, Feb 81 p 20

ABSTRACT: The basic theory of the electrolytic method of treating chromium-containing waste water is the fact that the positive iron plates or filings, under the action of electrical current, dissolve and produce ferrous ions; in the acid solution, the ferrous ions reduce the hexachromium into trichromium. As the electrolysis process proceeds, the pH of the treated water rises and the trichromium ions or trivalent iron ions precipitate as hydroxides, which are called, for the purpose of this paper, as electrolysis sludge. After electrolysis, the chromium-containing waste water of the record plant has reached the state's standard for discharge but the sludge becomes the problem. As chromium hydroxide is not dissolved in water or alcohol and the solubility of iron hydroxide is 2.85×10^5, the sludge is believed to be not harmful to humans. The current practice of mixing it with water to make a paste to be used as a wood filler and dressing on speaker boxes is described.

AUTHOR: None

ORG: Shanghai Jiading County Agricultural Machinery Repair Plant

TITLE: "The 285 Type High Speed Diesel Engine"

SOURCE: Shanghai JIXIE ZHIZAO [MECHANICAL ENGINEERING] in Chinese No 2, Feb 81 p 11, front cover

ABSTRACT: This paper explains the photo of the 285 type high speed diesel engine, which is reproduced on the front cover of this issue of the journal. This engine, belonging to the New 85 Series, is one of the multiple purpose small diesel engines developed in China in the 70's. It is light and reliable and easily repaired. A list of vehicles, agricultural machines, farm products processing machines, and pumps for which the engine is suitable is included. The paper also contains a brief description of its structure, property, and major technical specifications.

6248
CSO: 4009/230

Seismology

AUTHOR: LIU Guangyuan [0491 0342 6678]

ORG: Lanzhou Institute of Seismological Research, State's Bureau of Seismology

TITLE: "Pre-earthquake Long-Period Deformation Phenomena in the Crust"

SOURCE: Kunming DIZHEN YANJIU [JOURNAL OF SEISMOLOGICAL RESEARCH] in Chinese Vol 3 No 4, 80 pp 111-115

ABSTRACT: About 15 minutes before the occurrence of the 8.9 earthquake in Chile on 22 May 60, a strain gauge in Pasadena of the USA registered abnormal long-period waves of 300-600 sec. This is perhaps the long-period wave motion induced by preslip before the earthquake. Due to the fact that China did not have long-period seismograph, records of preslip of strong earthquakes were not obtained. In the past few years, the author and colleagues used geoinclinometers to proceed with observation and recorded some phenomena of long-period movements and occurrence of inclination of the crust toward the epicenter before some strong earthquakes. Metal horizontal pendulum inclinometers made in China were used in the observation. At present, this is a common method for detecting preearthquake signs. Some observed phenomena occurring shortly before earthquakes are introduced in the paper. This paper was received for publication on 12 Feb 80.

AUTHOR: ZHAO Genmo [6392 2704 2875]
WANG Junguo [3769 0193 0948]

ORG: Tianjin Municipal Bureau of Seismology

TITLE: "Precursory Earthquake Sequence of Some Chinese Strong Earthquakes"

SOURCE: Kunming DIZHEN YANJIU [JOURNAL OF SEISMOLOGICAL RESEARCH] in Chinese Vol 3 No 4, 80 pp 124-136

ABSTRACT: This paper proposes that before most strong earthquakes in China, 5 stages of graphic changes of regional earthquake activity occur in the following sequence: (1) Normal activity; (2) Preearthquake activity I; (3) Quiet --vacant region; (4) Preearthquake activity II; (5) Occurrence of the main earthquake. This is slightly more complex than the preearthquake sequence concept proposed by Aiweisun [transliteration; in Chinese translation of "A Short Discussion of Precursory Earthquake Sequence in Japan"] This paper compares the time of occurrence of precursory earthquake signs with the time of general precursory anomalies.

AUTHOR: WEI Pengfei [5898 7720 7378]

ORG: Tianjin Municipal Bureau of Seismology

TITLE: "Earthquake-absent Curves of North China"

SOURCE: Kunming DIZHEN YANJIU [JOURNAL OF SEISMOLOGICAL RESEARCH] in Chinese Vol 3 No 4, 80 pp 144-154

ABSTRACT: This paper reports a method created through the practice of earthquake monitoring and forecasting. Through an understanding of the principle of occurrence of a peak period of earthquake activity in North China, the earthquake-absent curves of the highest magnitude earthquakes Mmax-t are proposed following an analysis of b value and energy. The method of finding the curves and their significance are discussed. In practice, these curves correlate very well with modern occurrences of strong earthquakes in North China. They appear to be useful for forecasting and determining the tendency of earthquake activities.

6248
CSO: 4009/218

AUTHOR: GONG Jingming [7255 2417 2494]

ORG: None

TITLE: "Several Problems in Designing the Multiple-Point Displacement Meter for Measuring Rock Deformation Surrounding an Underground Chamber"

SOURCE: Chongqing DIXIA GONGCHENG [UNDERGROUND ENGINEERING] in Chinese No 2, 11 Feb 81 pp 1-3

ABSTRACT: It should be common knowledge that after excavation of an underground chamber, it is important to know the radial deformation characteristic of the rocks of various depths surrounding the chamber for the purpose of determining the external load and the support structure of the chamber, for monitoring safety, as well as for improving the traditional method of designing a cave. If the information of rock deformation characteristic is to be obtained, an instrument to measure the deformation of rocks of various depths must first be studied and made. At present, some countries have already produced these instruments, such as the disk type spring extensometer of the USA and other instruments of Italy, W. Germany, Australia, Pakistan, etc. In China, it was not until recent years that, based upon the needs of production, several research units began to study this type of instrument. This paper discusses several problems in designing a multiple-point displacement meter, based upon the experience in making the slip-resistance type multiple-point displacement meter and the differential transformer type multiple-point displacement meter. Required property, range of measurement, precision, and transmission component are among the problems discussed.

AUTHOR: GAO Eryang [7559 1422 3152]
ZHU Guilan [2612 2710 5695]

ORG: None

TITLE: "Using Convergence to Measure the Displacement of Surrounding Sides of a Tunnel"

SOURCE: Chongqing DIXIA GONGCHENG [UNDERGROUND ENGINEERING] in Chinese No 2, 11 Feb 81 pp 4-8

ABSTRACT: Dynamic morphological changes of adjoining rocks caused by the excavation of tunnels is a complex process and is related to many factors, including the geological condition, the construction method, the form of support, etc. The tendency in tunnel engineering technology is to design the support structure on the basis of measurement, which involves mainly measurement of displacement with mechanical instrument and installation, the most common instruments being single or multiple point rod displacement meter or convergence meter. The authors studied related foreign literatures to design and make the SWJ-78 Tunnel Sides displacement measurement instrument (a convergence meter). The structure of the instrument, its properties, and an analysis of results of test measurement using the instrument are reported.

AUTHOR: YANG Zhifa [2799 1807 3127]
LIU Zhuhua [0491 4554 5478]

ORG: None

TITLE: "Preliminary Application of the Displacement Reverse Analysis Method in Underground Engineering Designing"

SOURCE: Chongqing DIXIA GONGCHENG [UNDERGROUND ENGINEERING] in Chinese No 2, 11 Feb 81 pp 9-13

ABSTRACT: A reasonable estimate of ground stress and a measurement of various physical and mechanical indices of the rock body are extremely important for underground engineering design and a series of on site tests, consuming a great deal of manpower and materials are often required while these tests are often influenced by the petrographical structure, especially the soft and weak structural surface. An easily established, low cost, and reliable testing system is therefore needed and the displacement reverse analysis method is proposed under such a condition. It is a method of using the displacement data of actual measurement to calculate the modulus of elasticity of the surrounding rocks and the horizontal ground stress, and is thus called a reverse analysis method. Due to the fact that the authors adopt the graphic method as well as the results of displacement study in the finite-element method of underground engineering, the originally very complex 3-dimensional reverse analysis subject is simplified so that the modulus of elasticity of the surrounding rocks and the horizontal ground stress may be directly and quickly estimated on site. The method and its process of application are explained.

AUTHOR: ZHOU Ruiguang [0719 3843 0342]
LUO Guangwei [5012 0342 0251]
SHI Xizhong [4258 6932 1813]

ORG: None

TITLE: "Effect of the Direction of Arrangement of Caves on the Strength of the Rock Body and Its Destruction Mechanism"

SOURCE: Chongqing DIXIA GONGCHENG [UNDERGROUND ENGINEERING] in Chinese No 2, 11 Feb 81 pp 14-18

ABSTRACT: A laboratory rock body mechanical model experiment was carried out to study the effect of the direction of arrangement of underground caves on the deformation characteristic, the strength, and the destruction form of the rock body, i.e. the stability of the underground engineering project. The results demonstrate that when caves are arranged perpendicular to the direction of load, the modulus of deformation at peak strength is large and destruction is a tensile rupture; when they are parallel to the direction of load, the modulus of deformation is small and crack zones and planes are formed in mainly the same direction; when they are in a 45° angle with the direction of load, the modulus of deformation is even smaller, and shear destruction plane is formed in the direction of arrangement of the caverns.

6168
CSO: 4009/225

END

END OF

FICHE

DATE FILMED

May 19, 1981